Molecular Therapy
Nucleic Acids
Original Article

A Novel Single-Strand RNAi Therapeutic Agent Targeting the (Pro)renin Receptor Suppresses Ocular Inflammation

Atsuhiro Kanda,[1] Erdal Tan Ishizuka,[1] Atsushi Shibata,[2] Takahiro Matsumoto,[2] Hidekazu Toyofuku,[2] Kousuke Noda,[1] Kenichi Namba,[1] and Susumu Ishida[1]

[1]Laboratory of Ocular Cell Biology and Visual Science, Department of Ophthalmology, Faculty of Medicine and Graduate School of Medicine, Hokkaido University, Sapporo, Hokkaido 060-8638, Japan; [2]Division of Research and Development, BONAC Corporation, Fukuoka BIO Factory, Fukuoka 839-0861, Japan

The receptor-associated prorenin system (RAPS) refers to the pathogenic mechanism whereby prorenin binding to the (pro)renin receptor [(P)RR] dually activates the tissue renin-angiotensin system (RAS) and RAS-independent intracellular signaling. Here we revealed significant upregulation of prorenin and soluble (P)RR levels in the vitreous fluid of patients with uveitis compared to non-inflammatory controls, together with a positive correlation between these RAPS components and monocyte chemotactic protein-1 among several upregulated cytokines. Moreover, we developed a novel single-strand RNAi agent, proline-modified short hairpin RNA directed against human and mouse *(P)RR* [(P)RR-PshRNA], and we determined its safety and efficacy in vitro and in vivo. Application of (P)RR-PshRNA in mice caused significant amelioration of acute (uveitic) and chronic (diabetic) models of ocular inflammation with no apparent adverse effects. Our findings demonstrate the significant implication of RAPS in the pathogenesis of human uveitis and the potential usefulness of (P)RR-PshRNA as a therapeutic agent to reduce ocular inflammation.

INTRODUCTION

Inflammation is phylogenetically and ontogenetically the oldest defense system that is initiated by harmful irritation and environments such as infection and tissue injury.[1,2] On the other hand, pathogenic mechanisms associated with inflammatory reactions have been implicated in various diseases, including diabetes, cancer, and eye diseases.[3,4] In acute inflammation, leukocytes migrate to extravascular tissues to distinguish and eliminate the offending agent, mostly contributing to tissue repair. Conversely, in chronic inflammation, leukocytes cause damage to tissues because of continuous secretion of chemical mediators and toxic oxygen radicals, thereby leading to a functional maladaptation and tissue remodeling.[1,2] However, even in acute inflammation, excessive and repeated acute attacks can frequently lead to severe tissue damage and destruction. A growing body of evidence shows that inflammation plays a significant role in the pathogenesis of vision-threatening retinal diseases such as age-related macular degeneration and diabetic retinopathy,[3,4] in addition to the classic type of intraocular inflammation known as uveitis.

The renin-angiotensin system (RAS), an important controller of systemic blood pressure (circulatory RAS), plays distinct roles in inflammation and vascular abnormalities in various target tissues and organs (tissue RAS).[5,6] With regard to the relationship between the RAS and the eye, a pharmacological blockade of angiotensin-converting enzyme or angiotensin II type 1 receptor (AT1R) resulted in beneficial effects on the incidence and progression of diabetic retinopathy in several clinical trials.[7,8] In previous studies, we unraveled the molecular mechanisms in which the tissue RAS causes ocular inflammation in murine models of diabetes, uveitis, and choroidal neovascularization.[9–11]

Prorenin binding to (pro)renin receptor [(P)RR] causes a conformational change of the prorenin molecule to acquire renin enzymatic activity (i.e., nonproteolytic activation of prorenin),and thus triggers tissue RAS activation concurrently with (P)RR-mediated intracellular signal transduction. This dual activation of the tissue RAS and RAS-independent signaling pathways, referred to as the receptor-associated prorenin system (RAPS), was shown to be involved in the molecular pathogenesis of various vascular disorders such as inflammation and pathological angiogenesis.[12–17] Aliskiren, a direct renin inhibitor, competitively inhibited the renin enzymatic activity of both renin and activated prorenin via interaction with (P)RR in vitro; however, RAS inhibitors including aliskiren have no efficacy in blocking (P)RR's own downstream signals.[18] Interestingly, (P)RR undergoes cleavage by

Received 14 October 2016; accepted 1 January 2017;
http://dx.doi.org/10.1016/j.omtn.2017.01.001.

Correspondence: Susumu Ishida, Laboratory of Ocular Cell Biology and Visual Science, Department of Ophthalmology, Faculty of Medicine and Graduate School of Medicine, Hokkaido University, N-15, W-7, Kita-ku, Sapporo 060-8638, Japan.
E-mail: ishidasu@med.hokudai.ac.jp
Correspondence: Atsuhiro Kanda, Laboratory of Ocular Cell Biology and Visual Science, Department of Ophthalmology, Faculty of Medicine and Graduate School of Medicine, Hokkaido University, N-15, W-7, Kita-ku, Sapporo 060-8638, Japan.
E-mail: kanda@med.hokudai.ac.jp

Table 1. Clinical Characteristics of Patients with Uveitis

Case No.	Age (yr)	Sex	Clinical Diagnosis	Surgical Indication	Inflammatory Activity/ Steroid Use
1	63	female	sarcoidosis	ERM	quiescent
2	63	female	sarcoidosis	ERM	quiescent
3	76	male	sarcoidosis	ERM	quiescent
4	66	female	sarcoidosis	ERM	mild on PSL
5	59	female	sarcoidosis	ERM	quiescent
6	73	male	sarcoidosis	ERM	quiescent
7	78	female	sarcoidosis	VH/ERM	quiescent
8	81	female	sarcoidosis	VH	mild on PSL
9	60	female	sarcoidosis	MH	quiescent
10	35	female	sarcoidosis	ERM	mild
11	70	female	sarcoidosis	ERM	quiescent
12	62	female	sarcoidosis	ERM	quiescent
13	70	female	sarcoidosis	ERM	quiescent
14	44	female	sarcoidosis	ERM	quiescent
15	84	male	VKH	VMT	quiescent on PLS
16	83	female	uveitis of unknown origin	ERM	quiescent
17	60	female	uveitis of unknown origin	SRD	mild on PSL
18	72	female	uveitis of unknown origin	ERM	quiescent
19	78	female	uveitis of unknown origin	VH	mild on PSL
20	61	female	uveitis of unknown origin	ERM	mild
21	78	female	uveitis of unknown origin	VH	quiescent
22	65	female	uveitis of unknown origin	ERM	quiescent

ERM, epiretinal membrane; MH, macular hole; PSL, prednisolone; SRD, serous retinal detachment; VH, vitreous hemorrhage; VKH, Vogt-Koyanagi-Harada disease; VMT, vitreomacular traction.

proteases to generate a soluble form of (P)RR [s(P)RR] that retains its capability for nonproteolytic activation of prorenin, causing the conversion of angiotensin I from angiotensinogen in vitro.[19] In our recent reports, s(P)RR levels increased in the vitreous fluid of patients with proliferative diabetic retinopathy and correlated with vitreous levels of prorenin and vascular endothelial growth factor (VEGF).[20,21]

Thus, we hypothesize that suppressing RAPS by blocking prorenin-(P)RR interaction may result in beneficial effects on various vascular abnormalities represented by inflammation. In this study, we revealed a significant involvement of the RAPS in human uveitis, and we then designed a new class of single-strand RNAi molecule selectively targeting human and mouse *(P)RR* and confirmed its efficacy in suppressing ocular inflammation using acute (uveitic) and chronic (diabetic) models in mice.

RESULTS

Elevated Protein Levels of Prorenin and s(P)RR in Correlation with C-C Chemokine Ligand 2/Monocyte Chemotactic Protein-1 in Human Eyes with Uveitis

We previously reported that elevated s(P)RR is associated with VEGF-driven angiogenic activity in human diabetic retinopathy.[20,21] In addition to diabetic retinopathy, uveitis is also characterized by intraocular inflammation that leads to vision loss and blindness associated with occlusive retinal vasculitis, serous retinal detachment, secondary epiretinal membrane (ERM), and glaucoma in some severe cases. To investigate prorenin and s(P)RR involvement in uveitis, we performed ELISA experiments using vitreous aspirates from uveitic eyes and non-uveitic control eyes with idiopathic ERM and a macular hole (MH). The clinical diagnosis of uveitis in the present study included sarcoidosis, Vogt-Koyanagi-Harada (VKH) disease, and uveitis of unknown origin, which are the common etiologies of endogenous uveitis in Japan[22] (Table 1). Both the ligand and receptor proteins were detectable in all of the vitreous samples from uveitic and control eyes. Notably, RAPS components including prorenin, s(P)RR, and activated (i.e., receptor-associated) prorenin significantly increased in the vitreous fluid of uveitic eyes compared with controls (Table 2). Moreover, increased prorenin and s(P)RR levels were significantly correlated with each other ($p < 0.01$, $r^2 = 0.632$) (Figure 1A).

The vitreous levels of cytokines such as C-C chemokine ligand (CCL) 2/monocyte chemotactic protein (MCP)-1, interleukin (IL)-6, platelet-derived growth factor (PDGF)-BB, and VEGF-A, key molecules responsible for inflammation and neovascularization, were elevated in the eyes of patients with sarcoid uveitis.[23] To investigate the relationship between RAPS activation and ocular inflammation, we checked the protein levels of several cytokines in vitreous samples from our uveitic case series. Compared to control eyes, protein levels of CCL2/MCP-1, IL-6, PDGF-BB, and VEGF-A, but not tumor necrosis factor (TNF)-α or IL-1β, significantly increased in uveitic eyes (Table 2). Moreover, elevated CCL2/MCP-1 levels were significantly correlated with increased RAPS parameters, including (s)PRR ($p < 0.01$, $r^2 = 0.697$), prorenin ($p < 0.01$, $r^2 = 0.581$), and activated prorenin ($p < 0.01$, $r^2 = 0.669$) (Figures 1B–1D). These results indicate that the close link between the RAPS components and CCL2/MCP-1 levels would validate the pathogenic role of (P)RR that contributes to inflammation in human uveitis.

Structure and In Vitro Characterization of (P)RR-Proline-Modified Short Hairpin RNA

Based on our current (Figure 1) and previous findings,[12–17,20,21] a blockade of (P)RR is theorized to prevent the cascade of events essential in various vascular abnormalities represented by inflammation. To block the pathological function of (P)RR, we designed a new class of RNAi agent, proline-modified short hairpin RNA (PshRNA), to knockdown human and mouse *(P)RR/ATP6AP2* [i.e., (P)RR's gene name] mRNA. First, we performed in silico analysis regarding various parameters such as length, structure, sequence, and chemical and

Table 2. Vitreous Levels of RAPS Components and Various Cytokines

	Prorenin (pg/mL)	s(P)RR (ng/mL)	Activated Prorenin (fmol/L)	CCL. /MCP-1 (pg/mL)	IL-6 (pg/mL)	PDGF-BB (pg/mL)	VEGF-A (pg/mL)	TNF-α (pg/mL)	IL-1β (pg/mL)
ERM + MH (n = 13)	115.90 ± 15.17	4.96 ± 0.99	129.68 ± 37.34	1,396 ± 279.7	16.84 ± 6.86	3.64 ± 2.48	2.55 ± 0.29	0.24 ± 1.72	0.01 ± 0
Uveitis (n = 22)	187.29 ± 25.52	9.66 ± 1.07	391.83 ± 93.63	2,764 ± 322.1	72.57 ± 13.50	21.14 ± 5.13	37.69 ± 16.78	3.08 ± 0.78	0.03 ± 0.01
p value	0.022	0.003	0.015	0.005	0.001	0.007	0.028	0.622	0.058

Values are expressed as means ± SEM. ERM, epiretinal membrane; MH, macular hole.

nucleotide compositions, all of which mediate efficient RNAi,[24] and we generated five candidate RNAi agents targeting a different nucleotide sequence of the *(P)RR/ATP6AP2* gene (Table S1) common to both species. We then tested their knockdown efficiency in preliminary experiments (Figure S1) using human and mouse cell lines, so as to select one candidate (number 1) as (P)RR-PshRNA in terms of both potency and persistency of *(P)RR/ATP6AP2* knockdown. Figure 2A shows the base sequence and structure of (P)RR-PshRNA and (P)RR-small interfering RNA (siRNA).

Next, we investigated nuclease resistance to compare the RNA stability between the conventional siRNA and the newly designed PshRNA. Each RNAi was incubated in the presence of micrococcal nuclease and the degree of degradation was assessed over time. While (P)RR-siRNA was completely degraded after 5 min of incubation with micrococcal nuclease at 0.5 U, (P)RR-PshRNA was still intact after 30 min (Figure 2B), showing a more potent RNA stability in (P)RR-PshRNA. Incubation for 30 min with ≥3 U micrococcal nuclease showed (P)RR-PshRNA degradation (Figure 2C).

To determine how transfection with (P)RR-PshRNA inhibits the expression of *(P)RR/ATP6AP2* mRNA, in vitro studies with human retinal pigment epithelial (RPE) and mouse brain microvascular endothelial (bEnd.3) cell lines were carried out. Real-time RT-PCR showed that the levels of *(P)RR/ATP6AP2* mRNA significantly decreased following exposure to human RPE and mouse bEnd.3 cells with 0.01, 0.1, and 1 nM (P)RR-PshRNA as well as (P)RR-siRNA in a dose-dependent manner (Figures 2D and 2E). We further confirmed the knockdown efficiency of 1 nM (P)RR-PshRNA in protein expression levels by immunoblot analysis (Figures 2F and 2G).

Moreover, we investigated whether (P)RR-PshRNA affects off-target transcripts that have mismatches within the core sequence of (P)RR-PshRNA. There were no human or mouse mRNA sequences with one- or two-base mismatches hit by in silico analysis. Importantly, three (two human and one mouse) off-target transcripts containing three-base mismatches were found, but there was no significant effect on any of the three candidates (Figure S2).

Cell viability against an excessively high concentration of RNAi agents at 100 nM was examined to test their in vitro safety using human RPE and mouse bEnd.3 cells. There were no significant differences in cell viability among PBS, control-siRNA, (P)RR-siRNA, control-PshRNA, and (P)RR-PshRNA (Figure S3).

Tissue Distribution and In Vivo Safety of (P)RR-PshRNA

To determine tissue distribution of (P)RR-PshRNA injected into the vitreous cavity of murine eyes, we used tetramethylrhodamine (TAMRA)-labeled (P)RR-PshRNA. One hour after intravitreal injection at 100 pmol in 1 μL PBS, the labeled (P)RR-PshRNA signals were deeply penetrated and widely distributed to the ganglion cell layer, inner and outer nuclear layers, and RPE in the posterior segment of the eye and to the corneal epithelium and stroma in the anterior segment of the eye (Figures S4A–S4D). No signals were detected in eyes injected with non-labeled (P)RR-PshRNA (Figures S4E–S4H).

To evaluate the safety of (P)RR-PshRNA in retinal tissue, histological assessment was made with H&E-stained sections. The mouse retinas at 24 and 48 hr after intravitreal (P)RR-PshRNA injection at 100 pmol in 1 μL PBS appeared normal and did not differ from those of PBS-injected eyes (Figures 3A–3D). Next, we carried out electroretinography (ERG) for mice at 24 and 48 hr after intravitreal (P)RR-PshRNA injection to analyze its effect on retinal function (Figures 3E–3H). The mean amplitude values of a- and b-waves in eyes treated with (P)RR-PshRNA (at 24 hr: a-wave = 254.5 ± 23.1 μV and b-wave = 474.9 ± 29.2 μV; at 48 hr: a-wave = 317.7 ± 35.6 μV and b-wave = 631.8 ± 48.4 μV) were not significantly different from those of PBS-injected eyes (at 24 hr: a-wave = 275.7 ± 13.1 μV and b-wave = 490.1 ± 23.9 μV; at 48 hr: a-wave = 285.8 ± 29.1 μV and b-wave = 664.3 ± 48.1 μV; Figures 3I–3L).

To further explore the long-term safety of (P)RR-PshRNA to the mouse retina at 7 and 28 days after injection, these morphological and functional evaluations were repeated and terminal deoxynucleotidyl transferase-mediated digoxigenin-deoxyuridine nick-end labeling (TUNEL) assays were performed. Consistent with the short-term results (Figure 3), there were no differences in histology sections or in wave amplitudes between eyes treated with PBS and (P)RR-PshRNA at 7 and 28 days (Figure S5). TUNEL-positive cells were observed in the outer nuclear layer at 7 and 28 days after intravitreal injection with PBS or (P)RR-PshRNA at 100 pmol in 1 μL PBS, but no significant differences were detected (Figure S6).

Suppression of Cellular Responses by (P)RR-PshRNA in Acute Inflammation

The endotoxin-induced uveitis (EIU) model is frequently used as a model of acute inflammation in various organs, including the eye. We previously reported the significant suppression of intraocular

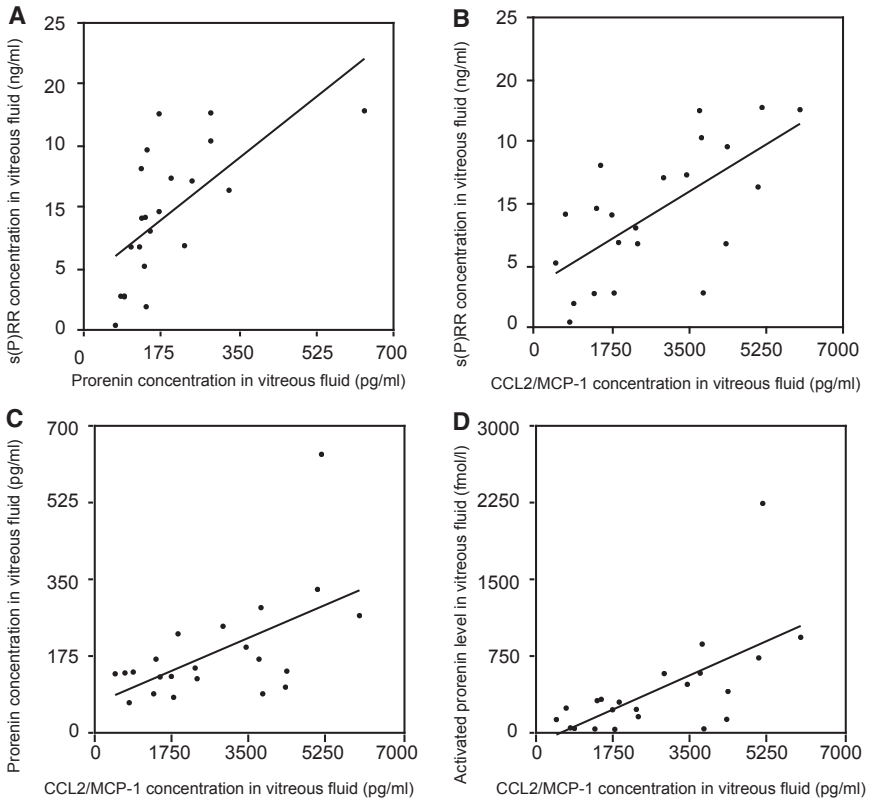

Figure 1. Elevated Protein Levels of Prorenin and s(P)RR in Correlation with CCL2/MCP-1 in Human Eyes with Uveitis

(A–D) Correlation between vitreous levels of s(P)RR and prorenin (A), s(P)RR and CCL2/MCP-1 (B), prorenin and CCL2/MCP-1 (C), and activated prorenin and CCL2/MCP-1 (D).

inflammation in this model by blocking AT1R and (P)RR to inhibit the tissue RAS and the RAPS, respectively.[11,15] To check the in vivo duration of knockdown efficiency, we measured retinal expression levels of *(P)RR/Atp6ap2* in EIU mice injected intravitreally with PBS or (P)RR-PshRNA at 100 pmol in 1 μL PBS, in comparison with untreated normal animals as controls (Figure S7). (P)RR-PshRNA-mediated suppression of *(P)RR/Atp6ap2* gene expression lasted up to 48 hr after (P)RR-PshRNA application (i.e., 24 hr after EIU induction), leading us to conduct the following in vivo inhibition experiments (Figures 4, 5, 6, S8, and S9) within the time window of 48 hr.

To examine whether intravitreal injection of (P)RR-PshRNA alters acute retinal inflammation, we evaluated the number of leukocytes adhering to retinal vessels in mice with EIU. Compared with control-PshRNA (324.9 ± 20.0 cells/retina), (P)RR-PshRNA administration led to a suppression of leukocyte adhesion in the EIU retina (223.1 ± 16.7 cells; Figures 4A–4E). To further confirm the inhibitory effect of (P)RR-PshRNA on acute retinal inflammation, we quantified the number of leukocytes infiltrating into the vitreous cavity adjacent to the optic disc in EIU mice. Leukocyte infiltration anterior to the optic disc, which markedly increased with induction of EIU, decreased with (P)RR-PshRNA treatment [control-PshRNA: 31.5 ± 3.8 cells; (P)RR-PshRNA: 14.0 ± 1.5 cells] (Figures 4F–4H).

Suppression of Molecular Responses by (P)RR-PshRNA in Acute Inflammation

To determine the molecular mechanisms in which *(P)RR* inhibition suppressed cellular responses in the EIU model (Figure 4), retinal mRNA expression of inflammatory genes was measured by real-time qPCR. Retinal mRNA levels of *Il-6*, *Ccl2/Mcp-1*, *Icam-1*, and *Tnf-α* were higher in EIU mice treated with PBS or control-PshRNA than in untreated normal animals used as controls. Intravitreal administration of (P)RR-PshRNA significantly reduced mRNA expression of these inflammatory molecules as well as *(P)RR/Atp6ap2* (Figure 5). These suppressive effects were observed in a dose-dependent manner (Figure S8).

Several reports showed that inflammatory signals in EIU caused excessive degradation of rhodopsin due to activation of the ubiquitin-proteasome system, leading to shortening of the rod photoreceptor outer segment (OS) length.[25,26] Treatment with (P)RR-PshRNA significantly prevented shortening of OS length and reduction of rhodopsin protein levels (Figure S9).

Suppression of Cellular and Molecular Responses by (P)RR-PshRNA in Chronic Inflammation

Streptozotocin (STZ)-induced diabetes is a model of type 1 diabetes due to impaired insulin secretion from pancreatic β cells injured by STZ toxicity. Given that diabetic retinopathy has recently been regarded as an inflammatory disorder, we used this model to study the effect of (P)RR-PshRNA on chronic inflammation (Figure 6) in contrast with acute inflammation in the EIU model (Figures 4 and 5). Using the STZ model, we previously showed that inhibition of AT1R and (P)RR decreased diabetes-induced retinal inflammation.[9,14] In this study, the total number of retinal adherent leukocytes significantly decreased in diabetic mice treated with (P)RR-PshRNA (17.9 ± 2.9 cells/retina) compared with control-PshRNA (45.0 ± 4.7 cells/retina) (Figures 6A–6E). Moreover, upregulated gene expression levels of *Il-6*, *Ccl2/Mcp-1*, *Icam-1*, *Tnf-α*, and *(P)RR/Atp6ap2*, as seen in diabetic mice treated with PBS or control-PshRNA, were significantly suppressed with administration of (P)RR-PshRNA (Figures 6F–6J).

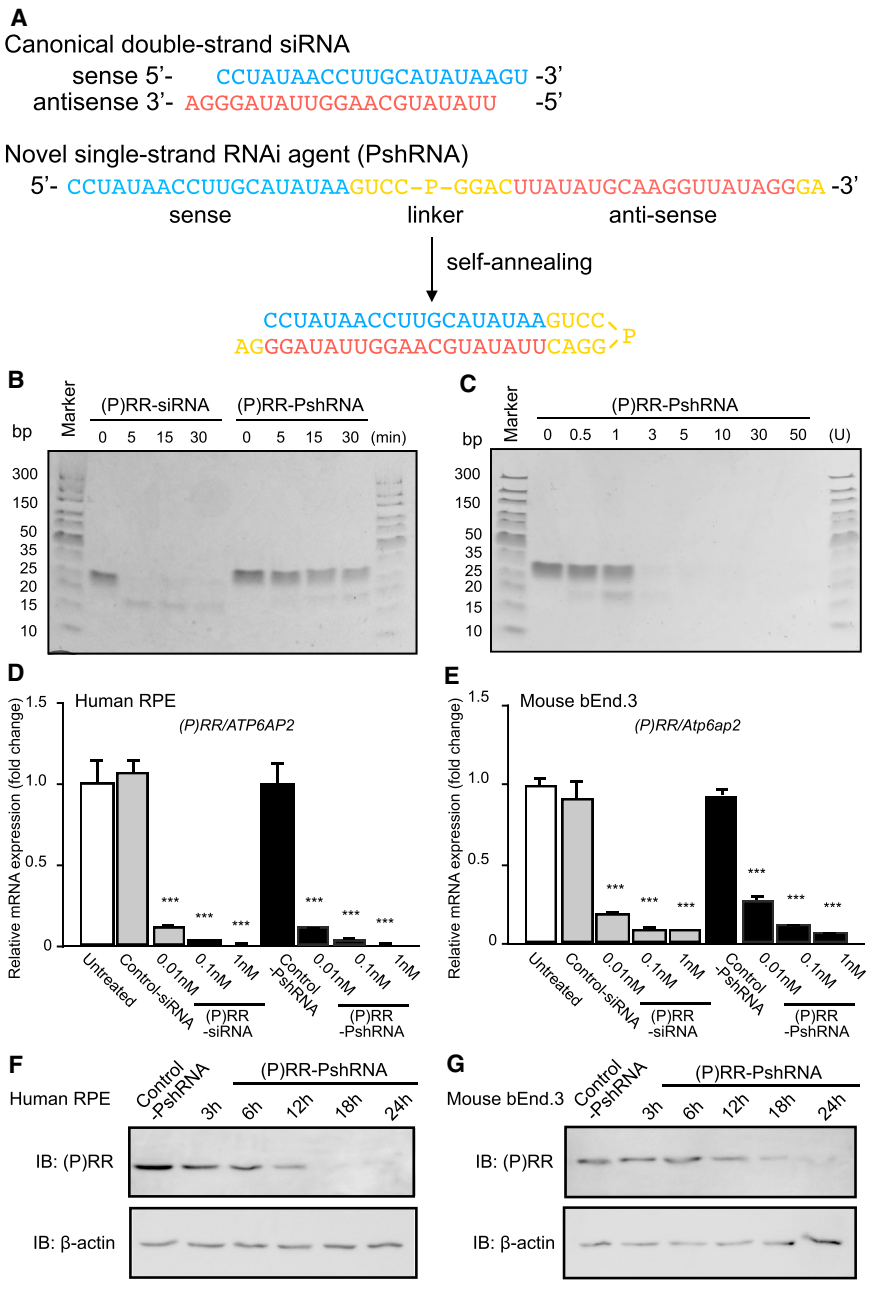

Figure 2. Structure and In Vitro Characterization of (P)RR-PshRNA

(A) Structure of canonical double-strand siRNA and novel single-strand RNAi (PshRNA) agents. Nucleotides in blue indicate the sense strand of the target [(P)RR/ATP6AP2], nucleotides in red are the antisense strand, and nucleotides in yellow are the linker region. P indicates a proline derivative. (B and C) Each RNAi agent was incubated in the presence of micrococcal nuclease and then separated on gel electrophoresis for incubation with 0.5 U enzyme for several durations (B) or with various units of enzyme for 30 min (C). (D and E) *(P)RR/ATP6AP2* mRNA expression levels in human RPE cells (D) and mouse endothelial cells (E) exposed to (P)RR-siRNA or (P)RR-PshRNA compared with control-siRNA or control-PshRNA, respectively (n = 8 per group). ***$p < 0.0001$. (F and G) Immunoblot analysis for (P)RR in human RPE cells (F) and mouse endothelial cells (G) transfected with control- or (P)RR-PshRNA.

DISCUSSION

The RNAi system has been used extensively for silencing the translation of an active gene and was recently applied to mammalian cells using siRNAs that are bound to the RNA-induced silencing complex, which mediate the cleavage of target mRNAs.[24,27] The present study reveals for the first time, to our knowledge, several important data on the involvement of RAPS in the inflammatory pathogenesis of human uveitis (Figure 1). Furthermore, we generated and characterized a novel class of single-strand RNAi (i.e., PshRNA) agent targeting human and mouse *(P)RR* (Figure 2), so as to suppress ocular inflammation in acute and chronic models (Figures 4, 5, and 6). Importantly, the newly designed (P)RR-PshRNA showed more robust nuclease resistance than the conventional double-strand (P)RR-siRNA (Figure 2) and did not affect retinal function and structure (Figure 3). Intravitreal (P)RR-PshRNA injection in mice significantly inhibited inflammatory cell adhesion and infiltration (Figures 4 and 6), together with underlying molecular mechanisms (Figures 5 and 6).

We previously revealed the significant contribution of the AT1R and (P)RR signaling pathways to upregulated expression of pathogenic molecules such as ICAM-1, IL-6, CCL2/MCP-1, and VEGF-A, and thus the association of RAS and RAPS with ocular inflammation and neovascularization in animal disease models and human clinical samples.[9–15,20,21,28,29] In our current study, we newly demonstrate elevated vitreous levels of prorenin and s(P)RR in patients with uveitis, as well as the significant correlation between these RAPS components and CCL2/MCP-1 levels. CCL2/MCP-1, a key mediator for leukocyte recruitment, was reported to increase in the vitreous fluid and aqueous humor in patients with uveitis.[23,30] A neutralizing antibody against CCL2/MCP-1 was shown to reduce pathological retinal neovascularization and inflammation.[31] Importantly, we previously indicated that RAS and RAPS blockade with AT1R blocker telmisartan and (P)RR blocker (PRRB), respectively, suppressed Ccl2/Mcp-1 protein and mRNA levels in murine models of ocular inflammation such as EIU and experimental autoimmune uveitis.[11,15,32] PRRB is also

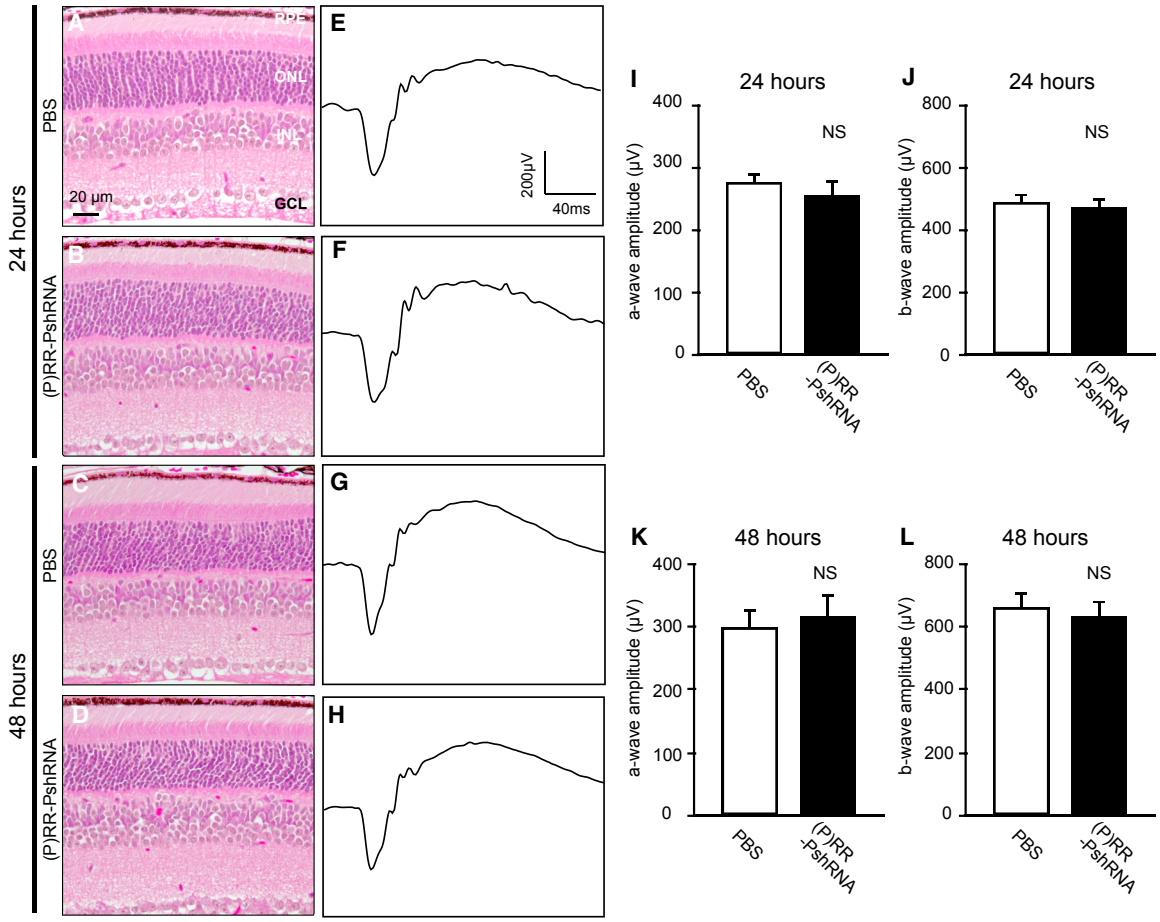

Figure 3. In Vivo Structural and Functional Safety of (P)RR-PshRNA

(A–D) Normal H&E staining of mouse retinas obtained at 24 and 48 hr after (P)RR-PshRNA or PBS treatment. Scale bar, 20 μm. (E–L) Scotopic ERG recordings at 24 and 48 hr after (P)RR-PshRNA or PBS treatment. There were no differences in the amplitudes of the a-wave and b-wave between eyes treated with PBS and (P)RR-PshRNA (n = 5–8 per group). GCL, ganglion cell layer; INL, inner nuclear layer; ONL, outer nuclear layer; NS, not significant; RPE, retinal pigment epithelial.

known as a handle-region peptide and has the structure of the handle region of the prorenin prosegment working as a decoy for (P)RR. PRRB is currently the only available agent to inhibit prorenin-(P)RR interaction (i.e., acquisition of renin enzymatic activity) leading subsequently to RAPS activation.[33] We and others have shown that PRRB potently suppresses the pathogenesis of various disease models in target organs (e.g., uveitis, age-related macular degeneration, retinopathy of prematurity, diabetic retinopathy, and nephropathy).[14,16,20,34] However, a blockade of ligand-receptor protein interaction using decoy peptides has several limitations, including (1) the requirement of an excessive amount of peptides, (2) induction of immune response and autoantibodies, (3) protease resistance, and (4) high molecular weight. These inherent and serious issues with decoy peptides are likely to preclude future clinical application.

RNAi is basically thought to have minimal cellular toxicity because of its endogenous cellular function for controlling gene expression, and it thus contains attractive and promising aspects for the development of new therapies. With regard to clinical application, however, there are some obstacles that must be overcome. In general, canonical double-strand siRNAs are recognized by family members of the Toll-like receptor (TLR) and retinoic acid-inducible gene I-like receptor, causing the activation of intracellular signaling pathways to initiate innate immunity.[35] Recently, a single-strand RNAi proved to be capable of sequence-specific gene silencing through the RNAi system without off-target expression of inflammatory cytokines via TLR-mediated signal transduction in rodent eyes.[36,37] Furthermore, although an annealing process is required for the generation of a double-strand siRNA, it is not necessary for a single-strand RNAi because the linker is replaced with proline derivatives and can therefore self-anneal. Previous studies showed that PshRNAs were more stable against nucleases than canonical double-strand siRNAs,[38,39] which is in agreement with our present data (Figure 2). Taken together, the single-strand RNAi strategy appears to overcome some of the drawbacks of canonical double-strand siRNAs.

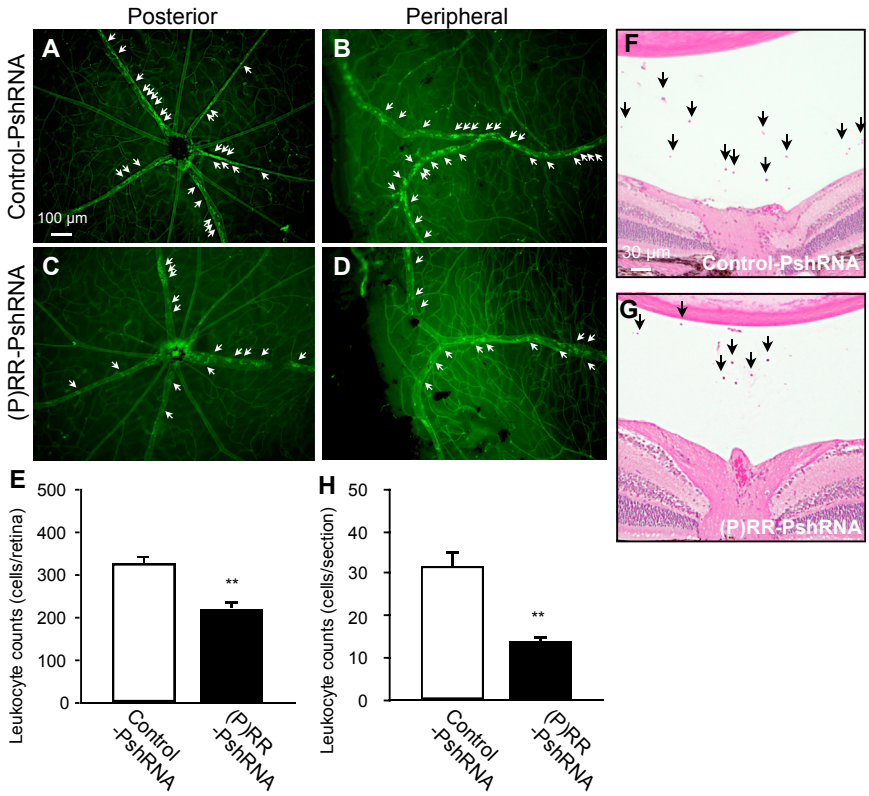

Figure 4. Suppression of Cellular Responses by (P)RR-PshRNA in Acute Inflammation

(A–D) Flatmounted retinas from EIU mice treated with control-PshRNA (A and B) or (P)RR-PshRNA (C and D). Arrows indicate firmly adhering leukocytes to the inflamed retinal vasculature. Scale bar, 100 μm. (E) Quantification of the number of retinal adherent leukocytes. **$p < 0.01$ ($n = 20–27$ per group). (F and G) Representative micrographs of leukocyte infiltration into the vitreous fluid of EIU mice treated with control-PshRNA (F) and (P)RR-PshRNA (G). Arrows indicate infiltrating leukocytes. Scale bar, 30 μm. (H) Quantification of the number of leukocytes in the vitreous fluid. **$p < 0.01$ ($n = 10–14$ per group).

(P)RR was originally found as an N-terminal truncated form of (P)RR, which is associated with vacuolar H^+-ATPase (v-ATPase) and thus was termed ATP6 accessory protein 2 (ATP6AP2).[40,41] Recently, several studies, including ours, using conditional knockout mice have revealed that (P)RR/Atp6ap2 contributes to physiologically essential cellular functions that are independent of RAPS.[42–45] In our current study, however, we did not observe any adverse events following application with (P)RR-PshRNA in vivo (Figures 3, S5, and S6) and in vitro (Figure S3). It is possible that the in vivo knockdown at the present dose of 100 pmol in 1 μL PBS per eye is too weak to cause any side effects, despite its significant efficacy in suppressing ocular inflammation (Figures 4, 5, 6 and S7–S9). Importantly, the currently designed sequence for RNAi targeting *(P)RR* is common to human and mouse genes, indicating that the multimodal animal testing with (P)RR-PshRNA would also serve as a useful reference for human clinical trials. Future studies are warranted to assess the long-term safety and efficacy of (P)RR-PshRNA in treating inflammation-related ocular disorders.

MATERIALS AND METHODS

Human Surgical Samples

Protein expression analysis of the vitreous fluid was performed on a total of 35 samples (22 cases and 13 controls). Based on international criteria, 14 patients (2 males and 12 females, average age = 64.3 ± 3.3 years) were diagnosed with sarcoidosis, 1 male patient (age = 84 years) had VKH disease, and 7 female patients (average age = 71.0 ± 3.5 years) had uveitis of unknown origin. The clinical characteristics of patients with uveitis are listed in Table 1. Control vitreous samples were obtained from 13 eyes of 13 non-uveitic patients (3 males and 10 females, average age = 66.8 ± 1.7 years) with idiopathic macular diseases, including ERM and MH. Undiluted vitreous samples were collected at the start of pars plana vitrectomy and were frozen rapidly at −80°C. This study was conducted in accordance with the tenets of the Declaration of Helsinki and was approved by the institutional review board of Hokkaido University Hospital. All patients gave written informed consent after we explained the purpose and procedures of this study.

ELISA

The protein levels of prorenin and s(P)RR in the vitreous fluid were determined with human prorenin (Innovative Research) and s(P)RR (Immuno-Biological Laboratories) ELISA kits per the manufacturers' instructions. Optical density was determined using a microplate reader (Sunrise; TECAN). Activated prorenin corresponds to prorenin bound with s(P)RR, and the dissociation constant (K_D) for the binding of prorenin with s(P)RR was calculated in a previous report[19] as follows: K_D (4.0 nmol/l) = [prorenin] × [s(P)RR]/[activated prorenin]. Based on the K_D, we determined the activated prorenin concentration in the vitreous fluid.

According a previous report[23] comparing the vitreous levels of cytokines between sarcoidosis and ERM, six cytokines were selected for measurement: CCL2/MCP-1, IL-6, PDGF-BB, VEGF-A, TNF-α, and IL-1β. Vitreous levels of the six cytokines were determined by using a commercially available multiplex bead analysis system (Multiplex-ELISA; Merck Millipore).

Generation of a New Class of RNAi Agent Targeting *(P)RR/ATP6AP2*

A new class of RNAi agent, PshRNA, was synthesized on a solid phase as a single-strand RNAi segment containing a short hairpin structure.

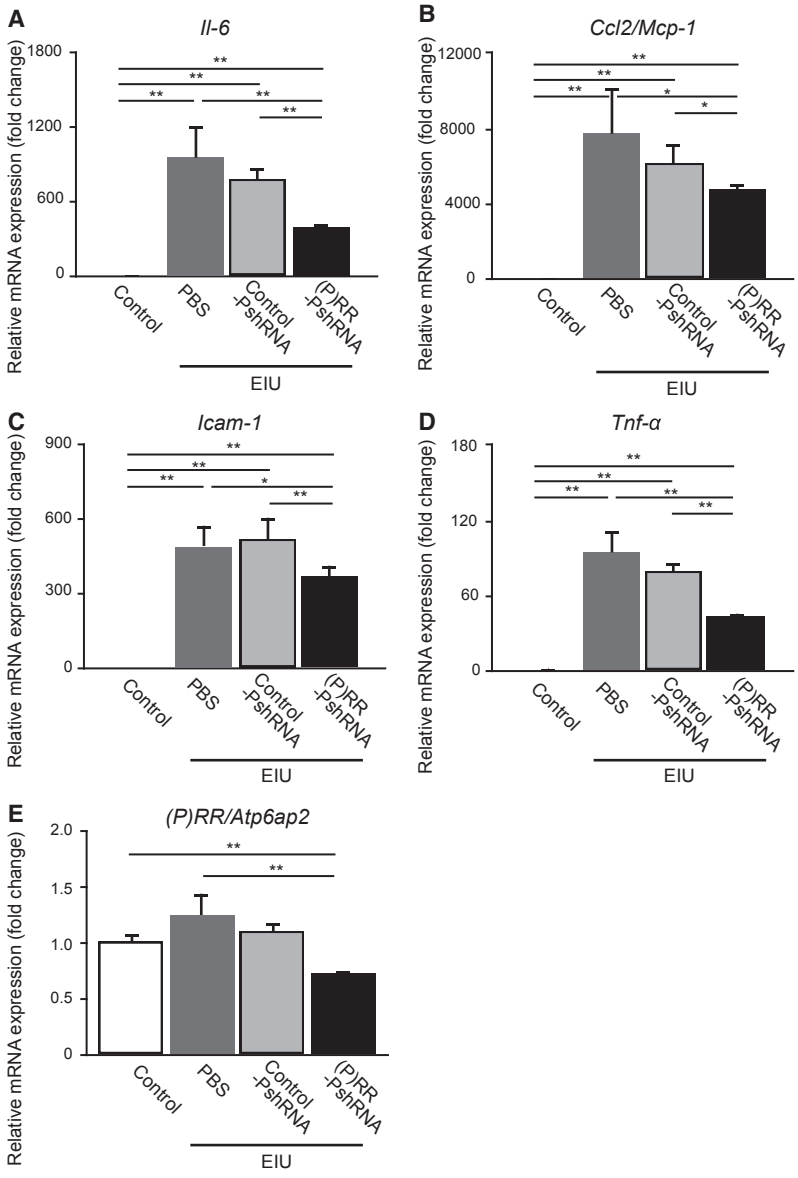

Figure 5. Suppression of Molecular Responses by (P)RR-PshRNA in Acute Inflammation

(A–E) Gene expression levels of inflammatory mediators *Il-6* (A), *Ccl2/Mcp-1* (B), *Icam-1* (C), and *Tnf-α* (D) and *(P)RR/Atp6ap2* (E) in retinas from untreated normal mice (control) and EIU mice treated with PBS, control-PshRNA, or (P)RR-PshRNA. *$p < 0.05$; **$p < 0.01$ ($n = 10$ per group).

The stem loop contains a proline derivative, as recently developed,[39] based on the strategy of creating PnkRNA (proline nick RNA).[38] We generated five candidate RNAi agents targeting a different nucleotide sequence of the *(P)RR/ATP6AP2* gene (Table S1) common to both human and mouse sequences. The 5′ region of (P)RR-PshRNA was attached with a fluorescent pigment TAMRA for drug delivery experiments. The negative control-PshRNA was 5′-UAC UAU UCG ACA CGC GAA GUU CC-P-GGA ACU UCG CGU GUC GAA UAG UAU U-3′, as recently established.[39]

(P)RR-siRNA was a canonical double-strand siRNA designed to target the same sequence with (P)RR-PshRNA. A negative control-siRNA oligo (SIC-001) was purchased from Sigma-Aldrich.

Evaluation of RNA Stability

To assess nuclease resistance for the evaluation of RNA stability, siRNA and PshRNA directed against *(P)RR* were incubated at 37°C with micrococcal nuclease (Takara Bio) as previously described.[38] After the specified times, nuclease reactions were stopped and the samples were run on a 15% Tris-borate-EDTA (TBE) gel. The gel was then stained with SYBR Safe (Life Technologies).

Cell Culture and Transfection

Human retinal pigment epithelial (hTERT-RPE1), mouse brain microvascular endothelial (bEnd.3), and mouse brain neuroblastoma (Neuro-2a) cells were obtained from American Type Culture Collection and cultured in DMEM/F12, DMEM, and Eagle's minimal essential medium (EMEM) (Wako Pure Chemical Industries), respectively, supplemented with 10% fetal bovine serum (Life Technologies) at 37°C and 5% CO_2. Cells were transfected with RNAi agents (0.01, 0.1, and 1 nM) using Lipofectamine RNAiMAX Reagent (Life Technologies).

Cellular viability was evaluated using Cell Counting Kit-8 (Dojindo) after cells were applied with RNAi agents (100 nM) for 24 hr, according to the manufacturer's protocol.

Animals and Drug Application

C57BL/6J mice aged 8–10 weeks (CLEA Japan) were maintained in the animal facility at Hokkaido University. Under deep anesthesia, control- or (P)RR-PshRNA was injected into the vitreous fluid. The dose of in vivo injection of control- or (P)RR-PshRNA was determined to be 100 pM in 1 μL PBS per eye, at which (P)RR-PshRNA significantly downregulated all of the inflammation-related molecules examined on top of *(P)RR/Atp6ap2* in dose-ranging experiments. All animal experiments were conducted in accordance with the Association for Research in Vision and Ophthalmology (ARVO) Statement for the Use of Animals in Ophthalmic and Vision Research and were approved by the Ethics Review Committee for Animal Experimentation of Hokkaido University.

Real-Time qPCR Analysis

Total RNA isolation and reverse transcription were performed using the SuperPrep Cell Lysis & RT Kit for qPCR (TOYOBO) with oligo

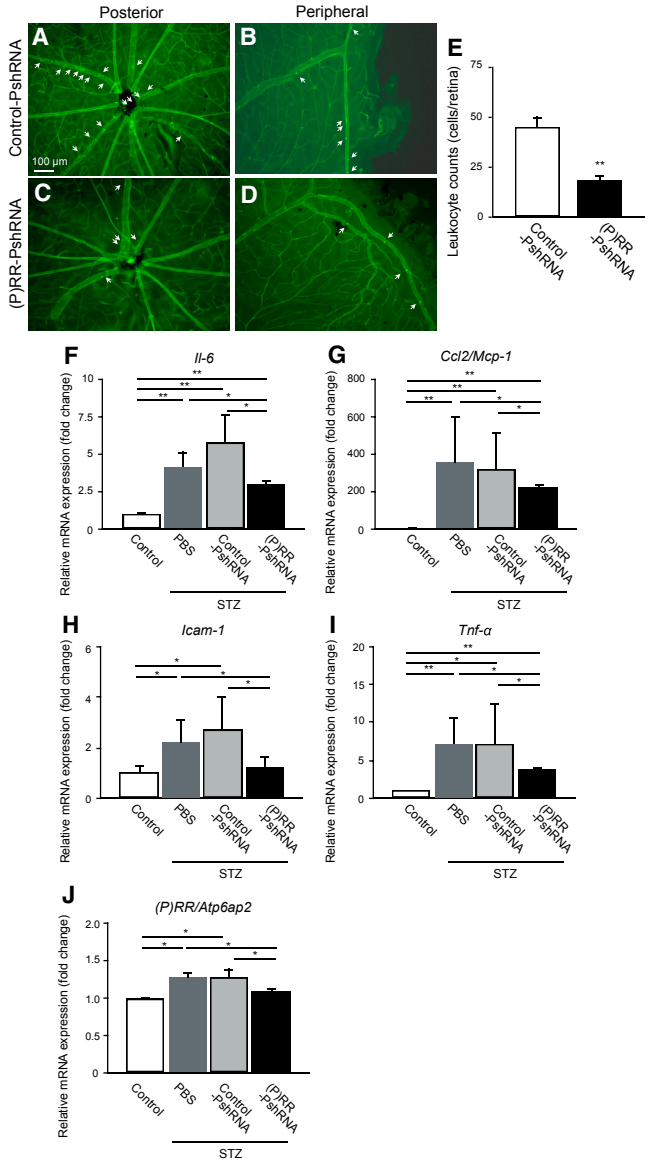

Figure 6. Suppression of Molecular Responses by (P)RR-PshRNA in Chronic Inflammation

(A–D) Flatmounted retinas from diabetic mice treated with control-PshRNA (A and B) or (P)RR-PshRNA (C and D). Scale bar, 100 μm. (E) The number of retinal adherent leukocytes. **p < 0.01 (n = 13–16 per group). (F–J) Gene expression levels of *Il-6* (F), *Ccl2/Mcp-1* (G), *Icam-1* (H), *Tnf-α* (I), and *(P)RR/Atp6ap2* (J) in retinas from untreated normal mice (control) and STZ-induced diabetes treated with PBS, control-PshRNA, or (P)RR-PshRNA. *p < 0.05; **p < 0.01 (n = 10–12 per group).

dT and random primers for cells and using TRIzol (Life Technologies) and GoScript Reverse Transcriptase (Promega) with oligo dT(20) primers for retinal tissues, as previously described.[20] Real-time qPCR was performed using GoTaq qPCR Master Mix (Promega) and the StepOne Plus System (Life Technologies). All primers are listed in Table S2. As for in vivo evaluation of pathogenic molecules, we selected four representative genes: *Il-6*, *Ccl2/Mcp-1*, *Icam-1*, and *Tnf-α*, all of which are known to be commonly involved in both acute and chronic inflammation models.[4,9,11,14,15,46]

Immunoblot Analysis

Cell and tissue extracts were lysed in SDS buffer and a protease inhibitor cocktail (Roche Applied Science). Proteins were resolved by 10% SDS-PAGE and transferred to polyvinylidene difluoride (PVDF) membrane (Merck Millipore) by electroblotting. Membranes were blocked in Tris-buffered saline (TBS) containing 5% skim milk and were incubated with the following primary antibodies: anti-(P)RR antibody (Sigma-Aldrich), anti-rhodopsin antibody (Merck Millipore), and anti-β-actin antibody (Medical & Biological Laboratories). The secondary antibodies for chemoluminescence detection were peroxidase-conjugated anti-mouse or anti-rabbit immunoglobulin Gs (IgGs) (Jackson ImmunoResearch Laboratories). The signal was obtained by enhanced chemoluminescence (Western Lightning Ultra; PerkinElmer).

ERG

ERG recordings were performed with a white light-emitting diode (LED) luminescent electrode placed on the cornea (PuREC system; Mayo). Mice were adapted to the dark overnight and were anesthetized under dim red light. The pupils were dilated with a mixed solution of 0.5% tropicamide and 0.5% phenylephrine (Mydrin-P; Santen). ERG was recorded at 1, 2, 7, and 28 days after the intravitreal injection of (P)RR-PshRNA. Eyes injected with PBS were used as control recordings. The scotopic ERG was elicited by a stimulus intensity of 10,000 cd m^{-2}, and the responses were differentially amplified and filtered between 0.3 and 300 Hz. Amplitudes were measured from baseline to the a-wave trough for a-waves and from the a-wave trough to the b-wave peak for b-waves.

Histological Sections and TUNEL Assay

For histological analysis, mouse eyes were fixed in 4% paraformaldehyde (PFA) at 4°C and then embedded in paraffin and sectioned. The sections were stained with H&E. To assess neuroprotection, photoreceptor outer segment lengths were measured in the posterior retina at four points (two points on either side of the optic nerve that were 200 and 500 μm apart), and averaged. The TUNEL assay was performed (Fluorescein Direct In Situ Apoptosis Detection Kit; Merck Millipore) to detect cleaved DNA in the paraffin-embedded sections, according to the manufacturer's instructions. Specimens were embedded in Frozen Section Compound (Leica) and cut into sections for drug delivery experiments. A Keyence BZ-9000 microscope was used for histological evaluation of the sections.

Induction of Acute and Chronic Inflammation Models

EIU and STZ-induced diabetes were used as acute and chronic inflammation models in mice. For the EIU model, mice were given an intraperitoneal injection of 0.2-mg lipopolysaccharide (LPS) from *Escherichia coli* (Sigma-Aldrich) 24 hr after an intravitreal injection of PBS, control-, or (P)RR-PshRNA. Mice were evaluated at 6 hr (for various gene expression) and 24 hr (for leukocyte adhesion and

infiltration, OS length shortening, and rhodopsin degradation) after LPS injection.

For the STZ model, animals received an intraperitoneal injection of STZ (Sigma) at a dose of 60 mg/kg body weight for 4 consecutive days. Animals with plasma glucose levels > 250 mg/dl at 7 days after injection were considered diabetic. After 2 months, animals received a single intravitreal injection of PBS, control-, or (P)RR-PshRNA. Mice were evaluated at 24 hr (for various gene expression) and 48 hr (for leukocyte adhesion) after the intravitreal injection.

Quantification of Retinal Adherent Leukocytes

The retinal vasculature and adherent leukocytes were imaged by perfusion labeling with fluorescein isothiocyanate (FITC)-coupled concanavalin A lectin (Con A; Vector Labs), as described previously.[46] Briefly, the chest cavity was opened and a cannula was introduced into the left ventricle under deep anesthesia. After injection of PBS to remove erythrocytes and non-adherent leukocytes, FITC-conjugated Con A was perfused. After the eyes were enucleated, the retinas were flatmounted. The flatmounts were visualized under a Keyence BZ-9000 microscope, and the total number of Con A-stained adherent leukocytes per retina was counted in a masked fashion.

Quantification of Vitreous Infiltrating Leukocytes

The number of leukocytes infiltrating into the vitreous cavity was analyzed as described previously.[46] Briefly, tissues were fixed and embedded in paraffin using standard techniques. Three 5-μm sections were prepared at a distance of 100 μm to each other, with the middle section passing through the optic nerve. All sections were stained with H&E, and the number of cells in the vitreous cavity was counted in a masked fashion.

Statistical Analyses

All results are expressed as means ± SEM. Statistical analyses were performed using the Student's t test, Mann-Whitney U test, or Spearman rank correlation. Differences were considered statistically significant when p values were < 0.05.

SUPPLEMENTAL INFORMATION

Supplemental Information includes nine figures and two tables and can be found with this article online at http://dx.doi.org/10.1016/j.omtn.2017.01.001.

AUTHOR CONTRIBUTIONS

A.K. and S.I. designed the study; A.K., E.T.I., A.S., T.M., S.T., K. Noda, and K. Namba performed the experiments; A.K., E.T.I., and S.I. analyzed the data; and A.K. and S.I. wrote the paper. All authors approved the final version submitted for publication.

CONFLICTS OF INTEREST

The authors declare no competing financial interests.

ACKNOWLEDGMENTS

We thank Ikuyo Hirose, Miyuki Murata, and Yoko Dong (Hokkaido University) for technical assistance. This work was supported in part by the New Energy and Industrial Technology Development Organization (NEDO), the Translational Research Network Program funded by the Japan Agency for Medical Research and Development (AMED) (to A.K.), the Takeda Science Foundation (to A.K.), the Japan Foundation for Applied Enzymology (to A.K.), the Institute of Science of Blood Pressure and Hormone (to A.K.), and the Ministry of Education, Science and Culture of Japan (grant-in-aid nos. 16K11279 to A.K. and 16H05484 to S.I.).

REFERENCES

1. Medzhitov, R. (2008). Origin and physiological roles of inflammation. Nature *454*, 428–435.
2. Medzhitov, R. (2010). Inflammation 2010: new adventures of an old flame. Cell *140*, 771–776.
3. Ambati, J., Anand, A., Fernandez, S., Sakurai, E., Lynn, B.C., Kuziel, W.A., Rollins, B.J., and Ambati, B.K. (2003). An animal model of age-related macular degeneration in senescent Ccl-2- or Ccr-2-deficient mice. Nat. Med. *9*, 1390–1397.
4. Joussen, A.M., Poulaki, V., Le, M.L., Koizumi, K., Esser, C., Janicki, H., Schraermeyer, U., Kociok, N., Fauser, S., Kirchhof, B., et al. (2004). A central role for inflammation in the pathogenesis of diabetic retinopathy. FASEB J. *18*, 1450–1452.
5. Ager, E.I., Neo, J., and Christophi, C. (2008). The renin-angiotensin system and malignancy. Carcinogenesis *29*, 1675–1684.
6. Paul, M., Poyan Mehr, A., and Kreutz, R. (2006). Physiology of local renin-angiotensin systems. Physiol. Rev. *86*, 747–803.
7. Chaturvedi, N., Porta, M., Klein, R., Orchard, T., Fuller, J., Parving, H.H., Bilous, R., and Sjølie, A.K.; DIRECT Programme Study Group (2008). Effect of candesartan on prevention (DIRECT-Prevent 1) and progression (DIRECT-Protect 1) of retinopathy in type 1 diabetes: randomised, placebo-controlled trials. Lancet *372*, 1394–1402.
8. Chaturvedi, N., Sjolie, A.K., Stephenson, J.M., Abrahamian, H., Keipes, M., Castellarin, A., Rogulja-Pepeonik, Z., and Fuller, J.H. (1998). Effect of lisinopril on progression of retinopathy in normotensive people with type 1 diabetes. The EUCLID Study Group. EURODIAB Controlled Trial of Lisinopril in Insulin-Dependent Diabetes Mellitus. Lancet *351*, 28–31.
9. Nagai, N., Izumi-Nagai, K., Oike, Y., Koto, T., Satofuka, S., Ozawa, Y., Yamashiro, K., Inoue, M., Tsubota, K., Umezawa, K., and Ishida, S. (2007). Suppression of diabetes-induced retinal inflammation by blocking the angiotensin II type 1 receptor or its downstream nuclear factor-kappaB pathway. Invest. Ophthalmol. Vis. Sci. *48*, 4342–4350.
10. Nagai, N., Oike, Y., Izumi-Nagai, K., Urano, T., Kubota, Y., Noda, K., Ozawa, Y., Inoue, M., Tsubota, K., Suda, T., and Ishida, S. (2006). Angiotensin II type 1 receptor-mediated inflammation is required for choroidal neovascularization. Arterioscler. Thromb. Vasc. Biol. *26*, 2252–2259.
11. Nagai, N., Oike, Y., Noda, K., Urano, T., Kubota, Y., Ozawa, Y., Shinoda, H., Koto, T., Shinoda, K., Inoue, M., et al. (2005). Suppression of ocular inflammation in endotoxin-induced uveitis by blocking the angiotensin II type 1 receptor. Invest. Ophthalmol. Vis. Sci. *46*, 2925–2931.
12. Satofuka, S., Ichihara, A., Nagai, N., Koto, T., Shinoda, H., Noda, K., Ozawa, Y., Inoue, M., Tsubota, K., Itoh, H., et al. (2007). Role of nonproteolytically activated prorenin in pathologic, but not physiologic, retinal neovascularization. Invest. Ophthalmol. Vis. Sci. *48*, 422–429.
13. Satofuka, S., Ichihara, A., Nagai, N., Noda, K., Ozawa, Y., Fukamizu, A., Tsubota, K., Itoh, H., Oike, Y., and Ishida, S. (2008). (Pro)renin receptor promotes choroidal neovascularization by activating its signal transduction and tissue renin-angiotensin system. Am. J. Pathol. *173*, 1911–1918.
14. Satofuka, S., Ichihara, A., Nagai, N., Noda, K., Ozawa, Y., Fukamizu, A., Tsubota, K., Itoh, H., Oike, Y., and Ishida, S. (2009). (Pro)renin receptor-mediated signal

transduction and tissue renin-angiotensin system contribute to diabetes-induced retinal inflammation. Diabetes *58*, 1625–1633.

15. Satofuka, S., Ichihara, A., Nagai, N., Yamashiro, K., Koto, T., Shinoda, H., Noda, K., Ozawa, Y., Inoue, M., Tsubota, K., et al. (2006). Suppression of ocular inflammation in endotoxin-induced uveitis by inhibiting nonproteolytic activation of prorenin. Invest. Ophthalmol. Vis. Sci. *47*, 2686–2692.
16. Ichihara, A., Hayashi, M., Kaneshiro, Y., Suzuki, F., Nakagawa, T., Tada, Y., Koura, Y., Nishiyama, A., Okada, H., Uddin, M.N., et al. (2004). Inhibition of diabetic nephropathy by a decoy peptide corresponding to the "handle" region for nonproteolytic activation of prorenin. J. Clin. Invest. *114*, 1128–1135.
17. Takahashi, H., Ichihara, A., Kaneshiro, Y., Inomata, K., Sakoda, M., Takemitsu, T., Nishiyama, A., and Itoh, H. (2007). Regression of nephropathy developed in diabetes by (Pro)renin receptor blockade. J. Am. Soc. Nephrol. *18*, 2054–2061.
18. Biswas, K.B., Nabi, A.H., Arai, Y., Nakagawa, T., Ebihara, A., Ichihara, A., Watanabe, T., Inagami, T., and Suzuki, F. (2010). Aliskiren binds to renin and prorenin bound to (pro)renin receptor in vitro. Hypertens. Res. *33*, 1053–1059.
19. Biswas, K.B., Nabi, A.N., Arai, Y., Nakagawa, T., Ebihara, A., Ichihara, A., Inagami, T., and Suzuki, F. (2011). Qualitative and quantitative analyses of (pro)renin receptor in the medium of cultured human umbilical vein endothelial cells. Hypertens. Res. *34*, 735–739.
20. Kanda, A., Noda, K., Saito, W., and Ishida, S. (2012). (Pro)renin receptor is associated with angiogenic activity in proliferative diabetic retinopathy. Diabetologia *55*, 3104–3113.
21. Kanda, A., Noda, K., Saito, W., and Ishida, S. (2013). Vitreous renin activity correlates with vascular endothelial growth factor in proliferative diabetic retinopathy. Br. J. Ophthalmol. *97*, 666–668.
22. Goto, H., Mochizuki, M., Yamaki, K., Kotake, S., Usui, M., and Ohno, S. (2007). Epidemiological survey of intraocular inflammation in Japan. Jpn. J. Ophthalmol. *51*, 41–44.
23. Nagata, K., Maruyama, K., Uno, K., Shinomiya, K., Yoneda, K., Hamuro, J., Sugita, S., Yoshimura, T., Sonoda, K.H., Mochizuki, M., and Kinoshita, S. (2012). Simultaneous analysis of multiple cytokines in the vitreous of patients with sarcoid uveitis. Invest. Ophthalmol. Vis. Sci. *53*, 3827–3833.
24. Elbashir, S.M., Harborth, J., Lendeckel, W., Yalcin, A., Weber, K., and Tuschl, T. (2001). Duplexes of 21-nucleotide RNAs mediate RNA interference in cultured mammalian cells. Nature *411*, 494–498.
25. Kamoshita, M., Ozawa, Y., Kubota, S., Miyake, S., Tsuda, C., Nagai, N., Yuki, K., Shimmura, S., Umezawa, K., and Tsubota, K. (2014). AMPK-NF-κB axis in the photoreceptor disorder during retinal inflammation. PLoS ONE *9*, e103013.
26. Ozawa, Y., Nakao, K., Kurihara, T., Shimazaki, T., Shimmura, S., Ishida, S., Yoshimura, A., Tsubota, K., and Okano, H. (2008). Roles of STAT3/SOCS3 pathway in regulating the visual function and ubiquitin-proteasome-dependent degradation of rhodopsin during retinal inflammation. J. Biol. Chem. *283*, 24561–24570.
27. Fire, A., Xu, S., Montgomery, M.K., Kostas, S.A., Driver, S.E., and Mello, C.C. (1998). Potent and specific genetic interference by double-stranded RNA in Caenorhabditis elegans. Nature *391*, 806–811.
28. Ishizuka, E.T., Kanda, A., Kase, S., Noda, K., and Ishida, S. (2014). Involvement of the receptor-associated prorenin system in the pathogenesis of human conjunctival lymphoma. Invest. Ophthalmol. Vis. Sci. *56*, 74–80.
29. Nagai, N., Noda, K., Urano, T., Kubota, Y., Shinoda, H., Koto, T., Shinoda, K., Inoue, M., Shiomi, T., Ikeda, E., et al. (2005). Selective suppression of pathologic, but not physiologic, retinal neovascularization by blocking the angiotensin II type 1 receptor. Invest. Ophthalmol. Vis. Sci. *46*, 1078–1084.
30. Valentincic, N.V., de Groot-Mijnes, J.D., Kraut, A., Korosec, P., Hawlina, M., and Rothova, A. (2011). Intraocular and serum cytokine profiles in patients with intermediate uveitis. Mol. Vis. *17*, 2003–2010.
31. Yoshida, S., Yoshida, A., Ishibashi, T., Elner, S.G., and Elner, V.M. (2003). Role of MCP-1 and MIP-1alpha in retinal neovascularization during postischemic inflammation in a mouse model of retinal neovascularization. J. Leukoc. Biol. *73*, 137–144.
32. Okunuki, Y., Usui, Y., Nagai, N., Kezuka, T., Ishida, S., Takeuchi, M., and Goto, H. (2009). Suppression of experimental autoimmune uveitis by angiotensin II type 1 receptor blocker telmisartan. Invest. Ophthalmol. Vis. Sci. *50*, 2255–2261.
33. Suzuki, F., Hayakawa, M., Nakagawa, T., Nasir, U.M., Ebihara, A., Iwasawa, A., Ishida, Y., Nakamura, Y., and Murakami, K. (2003). Human prorenin has "gate and handle" regions for its non-proteolytic activation. J. Biol. Chem. *278*, 22217–22222.
34. Kaneshiro, Y., Ichihara, A., Takemitsu, T., Sakoda, M., Suzuki, F., Nakagawa, T., Hayashi, M., and Inagami, T. (2006). Increased expression of cyclooxygenase-2 in the renal cortex of human prorenin receptor gene-transgenic rats. Kidney Int. *70*, 641–646.
35. Kleinman, M.E., Yamada, K., Takeda, A., Chandrasekaran, V., Nozaki, M., Baffi, J.Z., Albuquerque, R.J., Yamasaki, S., Itaya, M., Pan, Y., et al. (2008). Sequence- and target-independent angiogenesis suppression by siRNA via TLR3. Nature *452*, 591–597.
36. Takanashi, M., Sudo, K., Ueda, S., Ohno, S., Yamada, Y., Osakabe, Y., Goto, H., Matsunaga, Y., Ishikawa, A., Usui, Y., and Kuroda, M. (2015). Novel types of small RNA exhibit sequence- and target-dependent angiogenesis suppression without activation of Toll-like receptor 3 in an age-related macular degeneration (AMD) mouse model. Mol. Ther. Nucleic Acids *4*, e258.
37. Nakama, T., Yoshida, S., Ishikawa, K., Kobayashi, Y., Zhou, Y., Nakao, S., Sassa, Y., Oshima, Y., Takao, K., Shimahara, A., et al. (2015). Inhibition of choroidal fibrovascular membrane formation by new class of RNA interference therapeutic agent targeting periostin. Gene Ther. *22*, 127–137.
38. Hamasaki, T., Suzuki, H., Shirohzu, H., Matsumoto, T., D'Alessandro-Gabazza, C.N., Gil-Bernabe, P., Boveda-Ruiz, D., Naito, M., Kobayashi, T., Toda, M., et al. (2012). Efficacy of a novel class of RNA interference therapeutic agents. PLoS ONE *7*, e42655.
39. Taketani, Y., Usui, T., Toyono, T., Shima, N., Yokoo, S., Kimakura, M., Yamagami, S., Ohno, S., Onodera, R., Tahara, K., et al. (2016). Topical use of angiopoietin-like protein 2 RNAi-loaded lipid nanoparticles suppresses corneal neovascularization. Mol. Ther. Nucleic Acids *5*, e292.
40. Ludwig, J., Kerscher, S., Brandt, U., Pfeiffer, K., Getlawi, F., Apps, D.K., and Schägger, H. (1998). Identification and characterization of a novel 9.2-kDa membrane sector-associated protein of vacuolar proton-ATPase from chromaffin granules. J. Biol. Chem. *273*, 10939–10947.
41. Nguyen, G., Delarue, F., Burcklé, C., Bouzhir, L., Giller, T., and Sraer, J.D. (2002). Pivotal role of the renin/prorenin receptor in angiotensin II production and cellular responses to renin. J. Clin. Invest. *109*, 1417–1427.
42. Cruciat, C.M., Ohkawara, B., Acebron, S.P., Karaulanov, E., Reinhard, C., Ingelfinger, D., Boutros, M., and Niehrs, C. (2010). Requirement of prorenin receptor and vacuolar H+-ATPase-mediated acidification for Wnt signaling. Science *327*, 459–463.
43. Kanda, A., Noda, K., Yuki, K., Ozawa, Y., Furukawa, T., Ichihara, A., and Ishida, S. (2013). Atp6ap2/(pro)renin receptor interacts with Par3 as a cell polarity determinant required for laminar formation during retinal development in mice. J. Neurosci. *33*, 19341–19351.
44. Kinouchi, K., Ichihara, A., Sano, M., Sun-Wada, G.H., Wada, Y., Kurauchi-Mito, A., Bokuda, K., Narita, T., Oshima, Y., Sakoda, M., et al. (2010). The (pro)renin receptor/ATP6AP2 is essential for vacuolar H+-ATPase assembly in murine cardiomyocytes. Circ. Res. *107*, 30–34.
45. Kanda, A., Noda, K., and Ishida, S. (2015). ATP6AP2/(pro)renin receptor contributes to glucose metabolism via stabilizing the pyruvate dehydrogenase E1 β subunit. J. Biol. Chem. *290*, 9690–9700.
46. Kanda, A., Noda, K., Oike, Y., and Ishida, S. (2012). Angiopoietin-like protein 2 mediates endotoxin-induced acute inflammation in the eye. Lab. Invest. *92*, 1553–1563.